

# Turing patterns in systems with high-order interactions

Riccardo Muolo,<sup>1,2,\*</sup> Luca Gallo,<sup>1,3,\*</sup> Vito Latora,<sup>3,4,5</sup> Mattia Frasca,<sup>6,7</sup> and Timoteo Carletti<sup>1,2</sup>

<sup>1</sup>*naXys, Namur Institute for Complex Systems, University of Namur, Belgium*

<sup>2</sup>*Department of Mathematics, University of Namur, Belgium<sup>†</sup>*

<sup>3</sup>*Department of Physics and Astronomy & INFN, University of Catania, Italy*

<sup>4</sup>*School of Mathematical Sciences, Queen Mary University of London, UK*

<sup>5</sup>*Complexity Science Hub Vienna, Austria*

<sup>6</sup>*Department of Electrical, Electronics and Computer Science Engineering, University of Catania, Italy*

<sup>7</sup>*Istituto di Analisi dei Sistemi ed Informatica “A. Ruberti”,*

*Consiglio Nazionale delle Ricerche (IASI-CNR), Roma, Italy*

(Dated: July 11, 2022)

Turing theory of pattern formation is among the most popular theoretical means to account for the variety of spatio-temporal structures observed in Nature and, for this reason, finds applications in many different fields. While Turing patterns have been thoroughly investigated on continuous support and on networks, only a few attempts have been made towards their characterization in structures where high-order interactions are present. In this paper, we propose a generalization of reaction-diffusion systems to include many-body interactions, and we study their effects on the formation of Turing patterns. To achieve this goal, we rewrite the problem originally studied by Turing in a general form allowing for high-order terms and we prove that the interplay between the different orders of interaction may either enhance or repress the emergence of Turing patterns. Our results shed light on the mechanisms of pattern-formation in high-order structures and pave the way for further extensions of Turing original framework.

arXiv:2207.03985v1 [nlin.PS] 8 Jul 2022

---

\* These two authors contributed equally

<sup>†</sup> riccardo.muolo@unamur.be

## I. INTRODUCTION

Many natural and engineered systems exhibit collective behaviors, manifesting themselves as spatio-temporal ordered motifs, whose emergence can be explained utterly by considering the interactions within the system [1]. One of the most elegant and popular theories for the emergence of self-organized patterns is due to the British mathematician Alan Turing, who proposed, in the context of morphogenesis, a mechanism of pattern-formation rooted on a diffusion-driven instability, which now bears his name [2]. In a nutshell, the Turing instability results from the combined action of two processes, (local) reaction and (long-range) diffusion, involving an activator and an inhibitor species [3, 4]. While each process considered separately would drive the system to a spatially homogeneous state, there can be conditions on the models and on the interactions such that any heterogeneous, arbitrarily small, perturbation of the homogeneous state is amplified and eventually returns a macroscopic patchy (non-homogeneous) solution, i.e., a Turing pattern. The diffusive terms being the destabilizing factors, the above mechanism is also known in the literature as a diffusion-driven instability.

Despite its generality, the framework requires the involved species to diffuse with quite different rates, a condition that is not often naturally realized without introducing additional mechanisms, such as convection, electromagnetic fields, differential adherence. Indeed experimental evidence of the existence of Turing patterns was obtained almost half a century later in chemical reactions [5, 6] and in Cellular Neural Networks [7, 8]. Without adding unnecessary mechanisms and still looking for simple models, scholars have proposed several variants to the original Turing scheme to facilitate the emergence of patterns. For example, noise [9] or an upper bound to the signal propagation [10, 11] can be added to the picture.

In many relevant applications by their very definition, the local reactions involve very close species, that can thus be considered spatially separated from other groups. Starting from this observation Turing idea has been extended to discrete systems: species occupy spatially limited zones, i.e., nodes, and diffuse across links connecting different zones. Initially the theory has been developed as to include regular  $1D$  and  $2D$  lattices [12], and then on complex networks [13, 14].

The latter framework has proven particularly fruitful for Turing patterns, especially for the introduction of asymmetric displacements [15], as in the case of directed networks [16] or non-normal ones [17], where it was shown that Turing mechanism is enhanced. In particular, such framework is very general and allows to study the Turing instability on discrete topologies which are not trivially embedded on continuous domains, as it is the case for regular lattices. Nevertheless, certain dynamics escape the network framework, as the interactions between the elementary units are not only pairwise, but can be of higher-order, i.e., multi-body. One thus needs to resort to more sophisticated mathematical structures, such as hypergraphs and simplicial complexes, which are an extension of networks, beyond the framework of pairwise interactions [18, 19]. Dynamical systems on high-order topologies have been recently studied [20, 21], but a general theory of Turing pattern formation on top of such structures is still lacking. The aim of this paper is to fill this gap by proposing an extension of Turing instability on high-order topologies. For this scope, we will employ the formalism developed by Gambuzza et al. [21] in the context of synchronization.

By performing a linear stability analysis involving a high-order Laplace matrix and the Jacobian matrices of the reaction and coupling parts, we will show that the joint action of the high-order structures and the nonlinear interactions is the key feature in driving the systems unstable. Then, considering suitable choices of couplings and high-order topologies, we have analytically determined the conditions for the instability to occur by focusing on the role of the diffusion coefficients at every order; we will show that having different orders of diffusivities allows to enhance or reduce the formation of Turing patterns with respect to the pairwise setting, by tuning the parameters of the high-order couplings.

The paper is organized as follows. In the next section we will set the theoretical ground, by writing the equations originally studied by Turing, i.e., reaction-diffusion equations, for systems coupled through high-order structures. In section III, we will choose a particular kind of nonlinear coupling, namely the diffusive-like cubic one, and analyze the emergence of patterns for the sole pairwise interactions. In section IV, we will study the effects of high-order interactions on Turing instability: first with a particular kind of coupling, called natural coupling, which allows for an analytical formulation, showing that it is a generalization of some previous attempt to tackle the problem; then, we will examine an intermediate case, with some specific topologies, which we call regular topologies, also allowing for an analytical treatment, despite the relaxation of the natural coupling hypothesis; lastly, we will study the case with the most general coupling, fully exploiting the potential of high-order interactions, although only a numerical study is possible. Finally, in the last section, we will discuss further lines of investigation and possible applications.

## II. REACTION-DIFFUSION SYSTEMS ON HIGH-ORDER STRUCTURES

Let us consider a dynamical system composed by  $N$  identical units subject to some (local) nonlinear reaction dynamics. Assume moreover that many-body interactions, i.e., interactions in groups of more than two units, are allowed.

Let the state of the  $i$ -th unit to be described by the vector  $\vec{x}_i(t) \in \mathbb{R}^m$ , then, under the mentioned assumptions, the evolution

rate of the state vector of the  $i$ -th unit is governed by the following equation:

$$\dot{\vec{x}}_i = \vec{f}(\vec{x}_i) + \sum_{d=1}^P \sigma_d \sum_{j_1=1}^N \cdots \sum_{j_d=1}^N A_{i,j_1,j_2,\dots,j_d}^{(d)} \vec{g}^{(d)}(\vec{x}_i, \vec{x}_{j_1}, \vec{x}_{j_2}, \dots, \vec{x}_{j_d}) \quad (1)$$

with  $i = 1, \dots, N$ , where  $\vec{f}: \mathbb{R}^m \rightarrow \mathbb{R}^m$  describes the local nonlinear dynamics. Let  $P+1$  denote the size of the largest group of interacting units, then  $\vec{g}^{(d)}: \mathbb{R}^{m \times (d+1)} \rightarrow \mathbb{R}^m$ ,  $d \in \{1, \dots, P\}$ , are the nonlinear coupling functions ruling the  $(d+1)$ -body interactions, encoded into the adjacency tensors  $A^{(d)}$ , with  $A_{i,j_1,\dots,j_d}^{(d)} = 1$  if and only if the  $d+1$  units  $\{i, j_1, \dots, j_d\}$  interact together, i.e., they are connected by an hyperedge. We denote by  $\sigma_d > 0$  the coupling strengths. Let us assume the nonlinear couplings to be diffusive-like, hence for every  $d$  there exists a function  $\vec{h}^{(d)}(\vec{x}_{j_1}, \dots, \vec{x}_{j_d})$  such that  $\vec{g}^{(d)}$  can be written as:

$$\vec{g}^{(d)}(\vec{x}_i, \vec{x}_{j_1}, \dots, \vec{x}_{j_d}) = \vec{h}^{(d)}(\vec{x}_{j_1}, \dots, \vec{x}_{j_d}) - \vec{h}^{(d)}(\vec{x}_i, \dots, \vec{x}_i) \quad (2)$$

This definition of  $\vec{g}^{(d)}$  guarantees that the coupling vanishes when all units have the same state vector, namely  $\vec{g}^{(d)}(\vec{x}_i, \vec{x}_i, \dots, \vec{x}_i) = 0$ . If, in addition, we assume the existence of  $\vec{x}^* \in \mathbb{R}^m$  such that  $\vec{f}(\vec{x}^*) = 0$ , meaning that a solution of the  $N$  isolated systems exists, then it follows immediately from Eq. (2) that  $\vec{x}_i = \vec{x}^*$ , for all  $i = 1, \dots, N$ , i.e.,  $\vec{x}^*$  is a spatially independent solution of Eq. (1). This condition is a prerequisite for Turing instability that, as mentioned above, is based on the existence of a homogeneous stable equilibrium eventually destabilized by the diffusion. Notice that the diffusion terms are determined by the topology of the connections as well as by the parameters entering in the diffusive couplings, so that all these factors concurrently contribute to the mechanism of Turing pattern formation in the general model (1).

The standard framework to study Turing instability consists of two species reaction-diffusion systems. Let us thus set  $m = 2$  and denote the two components of the state vector  $\vec{x}_i$  by  $(u_i, v_i)$ . Then by defining  $\vec{f}(\vec{x}) = (f_1(u, v), f_2(u, v))$  and  $\vec{h}^{(d)}(\vec{x}_1, \dots, \vec{x}_d) = (h_1^{(d)}(u_1, \dots, u_d, v_1, \dots, v_d), h_2^{(d)}(u_1, \dots, u_d, v_1, \dots, v_d))$ , for all  $d = 1, \dots, P$ , we can rewrite Eq. (1) as

$$\begin{cases} \dot{u}_i = f_1(u_i, v_i) + \sum_{d=1}^P \sigma_d \sum_{j_1=1}^N \cdots \sum_{j_d=1}^N A_{i,j_1,\dots,j_d}^{(d)} \left[ h_1^{(d)}(u_{j_1}, \dots, u_{j_d}, v_{j_1}, \dots, v_{j_d}) - h_1^{(d)}(u_i, \dots, u_i, v_i, \dots, v_i) \right] \\ \dot{v}_i = f_2(u_i, v_i) + \sum_{d=1}^P \sigma_d \sum_{j_1=1}^N \cdots \sum_{j_d=1}^N A_{i,j_1,\dots,j_d}^{(d)} \left[ h_2^{(d)}(u_{j_1}, \dots, u_{j_d}, v_{j_1}, \dots, v_{j_d}) - h_2^{(d)}(u_i, \dots, u_i, v_i, \dots, v_i) \right] \end{cases} \quad (3)$$

where we have taken into account the condition (2). To focus on the role of high-order interactions, we can further simplify the model by assuming that the nonlinear diffusion does not contain any cross-diffusion term, namely for all  $d \in \{1, \dots, P\}$  the function  $h_1^{(d)}$  (resp.  $h_2^{(d)}$ ) depends only on  $\{u_{j_1}, \dots, u_{j_d}\}$  (resp.  $\{v_{j_1}, \dots, v_{j_d}\}$ ). Under this hypothesis, the examined system is for all  $i = 1, \dots, N$

$$\begin{cases} \dot{u}_i = f_1(u_i, v_i) + \sum_{d=1}^P \sigma_d \sum_{j_1=1}^N \cdots \sum_{j_d=1}^N A_{i,j_1,\dots,j_d}^{(d)} \left[ h_1^{(d)}(u_{j_1}, \dots, u_{j_d}) - h_1^{(d)}(u_i, \dots, u_i) \right] \\ \dot{v}_i = f_2(u_i, v_i) + \sum_{d=1}^P \sigma_d \sum_{j_1=1}^N \cdots \sum_{j_d=1}^N A_{i,j_1,\dots,j_d}^{(d)} \left[ h_2^{(d)}(v_{j_1}, \dots, v_{j_d}) - h_2^{(d)}(v_i, \dots, v_i) \right] \end{cases} \quad (4)$$

In the next sections, we will study the conditions for the emergence of Turing patterns in systems of the form (4) focusing, one-by-one, on the two novel aspects of our model. First, we will deal with the study of Turing patterns in the standard case when only two-body interactions are present (i.e., the model with  $P = 1$ ), but the diffusive coupling is nonlinear (Sec. III). Then, we will investigate the model in presence of multi-body nonlinear diffusive coupling (Sec. IV).

### III. TURING THEORY WITH NONLINEAR DIFFUSIVE-LIKE COUPLING

Let us start with the analysis of the conditions on the fixed point for the isolated system, that we here indicate as  $(u^*, v^*)$ . This means to only consider local reaction and silence the interactions among the different units. The fixed point satisfies the equations:

$$f_1(u^*, v^*) = f_2(u^*, v^*) = 0$$

and should be stable, a condition that can be obtained by imposing

$$\text{tr } \mathbf{J}_0 < 0 \text{ and } \det \mathbf{J}_0 > 0 \quad (5)$$

where  $\mathbf{J}_0 = \begin{pmatrix} \partial_u f_1 & \partial_v f_1 \\ \partial_u f_2 & \partial_v f_2 \end{pmatrix}$  is the Jacobian matrix of the reaction function, being  $\partial_a f_\ell = \frac{\partial f_\ell}{\partial a}(u^*, v^*)$ , with  $\ell \in \{1, 2\}$  and  $a \in \{u, v\}$ . Notice that all the derivatives in the Jacobian matrix are evaluated at the equilibrium point  $(u^*, v^*)$ .

Before studying the effects of high-order terms on the emergence of Turing patterns in the most general system in Eq. (4), let us first analyze the effect of a nonlinear diffusive coupling in a system with pairwise interactions only, i.e., when  $P = 1$ . This corresponds thus to consider a reactive system where nonlinear diffusion is present and interactions occur among units interacting in a complex network. Let us observe that the problem of Turing instability with nonlinear diffusion has already been studied on a continuous support for the dynamics [22–24]. The main purpose of the following sections is to extend this analysis to the case of networked systems and to introduce the reader to the framework of Turing theory on networks.

For sake of definitiveness, we will present our results by using a cubic diffusion term. We adopt the same assumption even in the case of high-order interactions, so that it will be easier to examine the effects of the latter on the dynamical behavior of the system.

### A. Turing patterns in networked systems with nonlinear diffusion

By setting  $P = 1$  in Eq. (4) we obtain

$$\begin{cases} \dot{u}_i = f_1(u_i, v_i) + \sigma_1 \sum_{j=1}^N A_{ij}^{(1)} (h_1^{(1)}(u_j) - h_1^{(1)}(u_i)) \\ \dot{v}_i = f_2(u_i, v_i) + \sigma_1 \sum_{j=1}^N A_{ij}^{(1)} (h_2^{(1)}(v_j) - h_2^{(1)}(v_i)) \end{cases} \quad \forall i = 1, \dots, N \quad (6)$$

These equations can be linearized around the the equilibrium point  $(u^*, v^*)$ , giving:

$$\begin{cases} \dot{\delta u}_i = \partial_u f_1(u^*, v^*) \delta u_i + \partial_v f_1(u^*, v^*) \delta v_i + \sigma_1 \sum_{j=1}^N A_{ij}^{(1)} \partial_u h_1^{(1)}(u^*) (\delta u_j - \delta u_i) \\ \dot{\delta v}_i = \partial_u f_2(u^*, v^*) \delta u_i + \partial_v f_2(u^*, v^*) \delta v_i + \sigma_1 \sum_{j=1}^N A_{ij}^{(1)} \partial_v h_2^{(1)}(v^*) (\delta v_j - \delta v_i) \end{cases} \quad (7)$$

where  $\delta u_i = u_i - u^*$ ,  $\delta v_i = v_i - v^*$  and  $i = 1, 2, \dots, N$ . Let  $L_{ij}^{(1)} = A_{ij}^{(1)} - k_i^{(1)} \delta_{ij}$  be the  $i, j$  element of the network Laplacian matrix<sup>1</sup>, where  $k_i^{(1)} = \sum_j A_{ij}^{(1)}$  is the node degree. We can rewrite the latter equation as

$$\frac{d}{dt} \begin{pmatrix} \delta u_i \\ \delta v_i \end{pmatrix} = \mathbf{J}_0 \begin{pmatrix} \delta u_i \\ \delta v_i \end{pmatrix} + \sigma_1 \sum_{j=1}^N L_{ij}^{(1)} \mathbf{J}_{H^{(1)}} \begin{pmatrix} \delta u_j \\ \delta v_j \end{pmatrix} \quad \forall i = 1, \dots, N \quad (8)$$

where  $\mathbf{J}_{H^{(1)}} = \begin{pmatrix} \partial_u h_1^{(1)}(u^*) & 0 \\ 0 & \partial_v h_2^{(1)}(v^*) \end{pmatrix}$ . Let us observe that matrix  $\mathbf{J}_{H^{(1)}}$  is diagonal, as there are no cross-diffusion terms. Let  $\vec{\xi} = (\delta u_1, \delta v_1, \dots, \delta u_N, \delta v_N)^T$  we can eventually rewrite the last equation in a compact form

$$\frac{d}{dt} \vec{\xi} = (\mathbb{I}_N \otimes \mathbf{J}_0 + \sigma_1 \mathbf{L}^{(1)} \otimes \mathbf{J}_{H^{(1)}}) \vec{\xi} \quad (9)$$

where  $\mathbb{I}_N$  is the  $N \times N$  identity matrix and  $\otimes$  is the Kronecker product.

The eigenvalues of the  $2N \times 2N$  linear system (9) determine the stability of the solution  $\vec{\xi}^* = 0$ , which corresponds to  $(u_i, v_i) = (u^*, v^*)$  for all  $i$ . Being  $\mathbf{L}^{(1)}$  a symmetric matrix, one can find a set of orthonormal eigenvectors  $\phi_\alpha^{(1)}$  associated to

<sup>1</sup> Let us observe that such matrix has a non positive spectrum and it is the discrete analogous of the continuous diffusion operator  $\nabla^2$  once the underlying network is a regular lattice; for this reason, the network Laplacian matrix plays a relevant role in the context of Turing pattern formation. However, we would like to point out that in the literature it is common to find the Laplacian matrix defined as  $L_{ij}^{(1)} = k_i^{(1)} \delta_{ij} - A_{ij}^{(1)}$  (e.g., [21, 25]), having thus a non negative spectrum. Then in such cases the coupling term will exhibit a negative sign.

eigenvalues  $\Lambda_\alpha^{(1)}$ ,  $\alpha = 1, \dots, N$ . We can then make one step further by projecting (9) onto this basis, and thus obtaining  $N$  linear and decoupled  $2 \times 2$  systems, each one depending on a single eigenvalue, namely

$$\frac{d}{dt} \begin{pmatrix} \delta \hat{u}_\alpha \\ \delta \hat{v}_\alpha \end{pmatrix} = [\mathbf{J}_0 + \sigma_1 \Lambda_\alpha^{(1)} \mathbf{J}_{H^{(1)}}] \begin{pmatrix} \delta \hat{u}_\alpha \\ \delta \hat{v}_\alpha \end{pmatrix} := \mathbf{J}^{(\alpha)} \begin{pmatrix} \delta \hat{u}_\alpha \\ \delta \hat{v}_\alpha \end{pmatrix} \quad \forall \alpha = 1, \dots, N \quad (10)$$

Here  $\delta \hat{u}_\alpha = \sum_i \delta u_i \phi_{\alpha,i}^{(1)}$  and  $\delta \hat{v}_\alpha = \sum_i \delta v_i \phi_{\alpha,i}^{(1)}$ , are the projection respectively of  $\delta u_i$  and  $\delta v_i$  on such eigenbasis, and the last equality defines the matrix  $\mathbf{J}^{(\alpha)}$ . Its eigenvalues can be obtained by solving

$$\det(\mathbf{J}^{(\alpha)} - \lambda \mathbb{I}_2) = 0$$

that is

$$\lambda^2 - 2\text{tr } \mathbf{J}^{(\alpha)} \lambda + \det \mathbf{J}^{(\alpha)} = 0$$

The root with the largest real part, considered as a function of  $\Lambda_\alpha^{(1)}$ , is named dispersion relation,  $\lambda_\alpha = \max \lambda(\Lambda_\alpha^{(1)})$ . If there exists  $\hat{\alpha}$  such that  $\lambda_{\hat{\alpha}} > 0$ , then the equilibrium solution  $(u_i, v_i) = (u^*, v^*)$  is unstable and a Turing instability is observed, the system drives away from the homogeneous equilibrium to eventually reach a new, possibly heterogeneous, solution.

Let us observe that  $\text{tr } \mathbf{J}^{(\alpha)} = \text{tr } \mathbf{J}_0 + \Lambda_\alpha^{(1)} \text{tr } \mathbf{J}_H$ . Because  $h_1$  and  $h_2$  encode a diffusive coupling, one can safely assume that  $\partial_u h_1(u^*) > 0$  and  $\partial_v h_2(v^*) > 0$ , moreover being  $\Lambda_\alpha^{(1)} \leq 0$  and  $\text{tr } \mathbf{J}_0 < 0$ , one can conclude that  $\text{tr } \mathbf{J}^{(\alpha)} < 0$  for all  $\alpha$ . In conclusion, a sufficient condition to have  $\lambda_{\hat{\alpha}} > 0$  results to be

$$\det \mathbf{J}^{(\hat{\alpha})} < 0 \quad (11)$$

for some  $\hat{\alpha} > 1$ .

## B. The Brusselator model with cubic diffusion

For sake of simplicity and without loss of generality, let us illustrate the above results assuming as reaction part the Brusselator model [26, 27], an extensively adopted dynamical system, when it comes to study the emergence of self-organized patterns. In addition, let us consider a cubic diffusion term. This accounts to set

$$\begin{aligned} f_1(u, v) &= 1 - (b+1)u + cu^2v \\ f_2(u, v) &= bu - cu^2v \end{aligned} \quad (12)$$

and

$$\begin{aligned} h_1^{(1)}(u) &= D_u^{(1)} u^3 \\ h_2^{(1)}(v) &= D_v^{(1)} v^3 \end{aligned} \quad (13)$$

where  $b$  and  $c > 0$  are model parameters,  $D_u^{(1)} > 0$  and  $D_v^{(1)} > 0$  sort of generalized diffusion coefficients. Hence, the system under investigation reads:

$$\begin{cases} \dot{u}_i = 1 - (b+1)u_i + cu_i^2v_i + \sigma_1 D_u^{(1)} \sum_{j=1}^N A_{ij_1}^{(1)} (u_{j_1}^3 - u_i^3) \\ \dot{v}_i = bu_i - cu_i^2v_i + \sigma_1 D_v^{(1)} \sum_{j=1}^N A_{ij_1}^{(1)} (v_{j_1}^3 - v_i^3) \end{cases} \quad (14)$$

for which it is straightforward to show the existence of a unique fixed point  $(u^*, v^*) = (1, b/c)$ . Correspondingly, the matrices  $\mathbf{J}_0$  and  $\mathbf{J}_{H^{(1)}}$  are:

$$\mathbf{J}_0 = \begin{bmatrix} b-1 & c \\ -b & -c \end{bmatrix} \quad \text{and} \quad \mathbf{J}_{H^{(1)}} = 3 \begin{bmatrix} (u^*)^2 D_u^{(1)} & 0 \\ 0 & (v^*)^2 D_v^{(1)} \end{bmatrix}. \quad (15)$$

Thus, the equilibrium  $(u^*, v^*)$  is stable provided that  $\text{tr } \mathbf{J}_0 = b - c - 1 < 0$  and  $\det \mathbf{J}_0 = c > 0$ . The conditions (11) for the onset of the instability are given by:

$$\begin{cases} -c^3 D_u^{(1)} + (b-1)b^2 D_v^{(1)} > 0 \\ 4b^2 c D_u^{(1)} D_v^{(1)} - (-c^3 D_u^{(1)} + (b-1)b^2 D_v^{(1)})^2 < 0 \end{cases} \quad (16)$$

Let us observe that the above conditions do not depend on  $\sigma_1$ . As in the case of Turing instability resulting from linear diffusion, the relevant parameter is the ratio between the diffusive coefficients.

In Fig. 1 we compare the Turing instability regions (i.e., the set of parameters for which Turing patterns can emerge) obtained in the case of a linear diffusion term and in the case of a cubic one. By fixing in both cases the diffusion coefficients  $D_u^{(1)} = 0.1$  and  $D_v^{(1)} = 1.0$ , and the coupling strength  $\sigma_1 = 1.0$ , we can observe the following behavior in the plane  $(b, c)$ . The instability region is wider in the case of linear coupling than in the cubic one for large values of the parameters, while the instability region shrinks to zero more slowly in the case of cubic coupling for small values of the parameters. This implies that for large enough values of  $b$  and  $c$  the linear diffusion allows the emergence of Turing patterns, while in the case of cubic diffusion any initial perturbation about the homogeneous equilibrium fades out. On the contrary, if  $b$  and  $c$  are small enough, Turing patterns can emerge under the assumption of cubic diffusion but not if diffusion is linear. These considerations are confirmed by the dispersion relation as reported in the left panels of Fig. 1: the reader can clearly identify the existence of eigenmodes associated to a positive dispersion relation for the cubic diffusion case (upper panel), while under the assumption of linear diffusion the dispersion relation is always negative, or the opposite case (bottom panel) where is the dispersion curve associated to nonlinear diffusion to be always negative. Let us remark that the spectrum of the Laplacian  $\Lambda^{(\alpha)}$  is discrete, however in order to help the reader to better visualize the results the dispersion relations are plotted also as continuous curves.

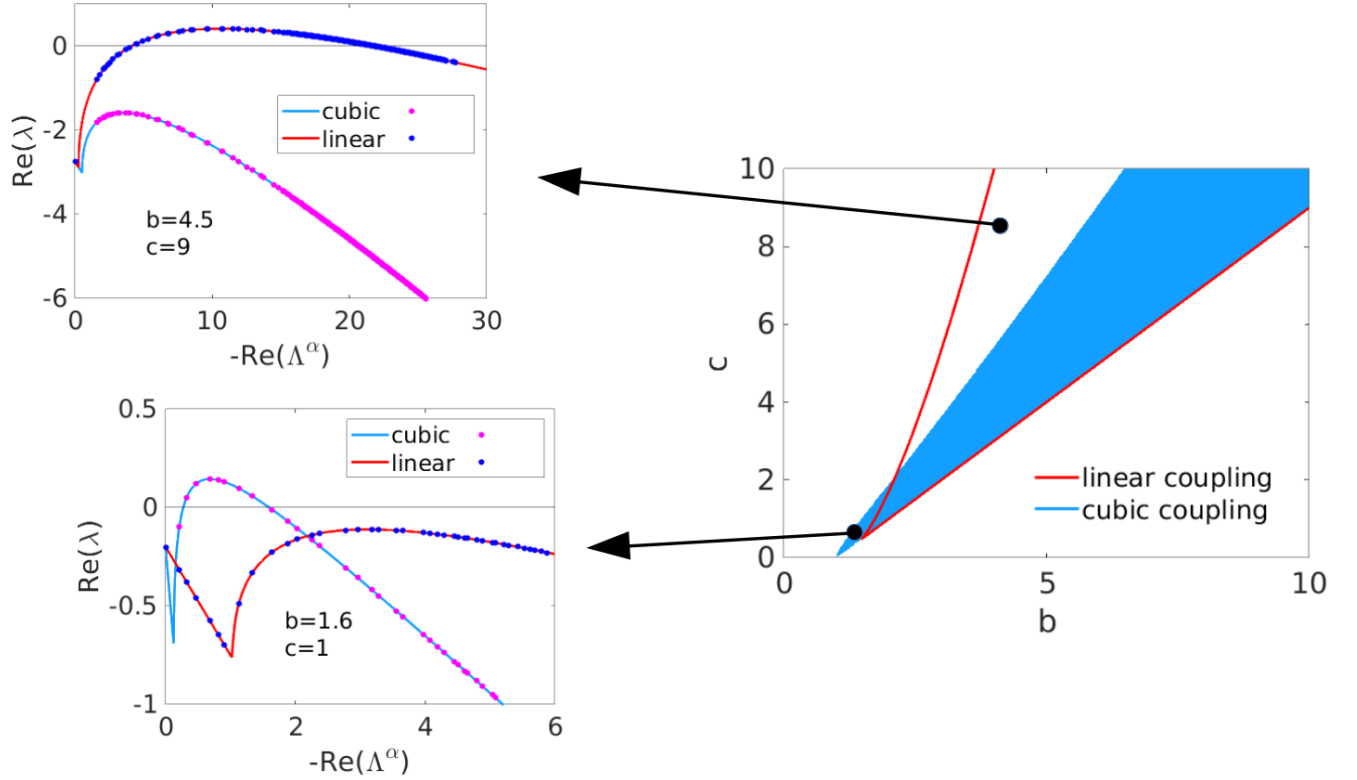


Figure 1. *Turing instability in networks with nonlinear diffusion.* Right panel: Turing instability regions for the Brusselator model with  $D_u^{(1)} = 0.1$ ,  $D_v^{(1)} = 1$  and  $\sigma_1 = 1$ . The analytical red curves indicate the instability regions for the linear coupling, while the blue region is for the cubic coupling, as obtained numerically. We can observe that, for lower values of the parameters  $(b, c)$  the cubic coupling allows for pattern formation, where the linear one does not, while for greater values we find the opposite situation. This can be visualized through the dispersion relations reported in the left panels: on the bottom left for lower values of the parameter (only the system subject to cubic coupling can go unstable), while on the upper left for greater values of the parameter (only the linear case yields patterns).

Let us conclude this section by observing that the standard Turing framework of linear Fickian diffusion, operating both with networks or continuous supports, requires the activator species to diffuse faster than the inhibitor one [3], i.e.,  $D_v^{(1)} > D_u^{(1)}$ . With the introduction of nonlinear diffusion, such condition can be relaxed, as the system can yield patterns even with equal diffusivities or with faster activator [22]. This claim follows directly from conditions (16) for the specific case of the Brusselator model. However, it is important to note that if one considers the entries of  $J_{H^{(1)}}$  as the "effective" diffusion coefficients, one finds a generalization of the Turing condition  $D_v^{(1)} > D_u^{(1)}$ , which is

$$(v^*)^2 D_v^{(1)} > (u^*)^2 D_u^{(1)} \quad (17)$$

for the cubic case. In fact, conditions (5) and (11) imply that  $\partial_u f_1 < |\partial_v f_2|$ , from which we obtain

$$\partial_u f_1 (v^*)^2 D_v^{(1)} > \partial_v f_2 (u^*)^2 D_u^{(1)} \Rightarrow \partial_u f_1 (v^*)^2 D_v^{(1)} > |\partial_v f_2| (u^*)^2 D_u^{(1)} > \partial_u f_1 (u^*)^2 D_u^{(1)}$$

hence the new condition  $(v^*)^2 D_v^{(1)} > (u^*)^2 D_u^{(1)}$ .

In the following, we will make use of the above results and focus our attention on the impact of high-order terms on the onset of the instability. The nonlinear coupling is necessary to make such many-body interactions meaningful, as pointed out in [28]: in fact, if the high-order coupling is linear, high-order interactions are nothing more than the sum of pairwise ones. Moreover, nonlinear couplings are of particular physical interest, as they are associated to anomalous diffusion [29].

#### IV. HIGH-ORDER INTERACTIONS

Let us now consider the most general case of Eq. (4) with high-order interactions. For simplicity and without loss of generality, we will limit ourselves to consider only first and second order interactions, i.e.,  $P = 1$  and  $P = 2$ . Nevertheless, the theory goes beyond the exposed examples and can be straightforwardly generalized as to include higher  $P$ . The system we are thus interested in is given by

$$\begin{cases} \dot{u}_i = f_1(u_i, v_i) + \sigma_1 D_u^{(1)} \sum_{j_1=1}^N A_{ij_1}^{(1)} (h_1^{(1)}(u_{j_1}) - h_1^{(1)}(u_i)) \\ \quad + \sigma_2 D_u^{(2)} \sum_{j_1=1}^N \sum_{j_2=1}^N A_{ij_1 j_2}^{(2)} (h_1^{(2)}(u_{j_1}, u_{j_2}) - h_1^{(2)}(u_i, u_i)) \\ \dot{v}_i = f_2(u_i, v_i) + \sigma_1 D_v^{(1)} \sum_{j_1=1}^N A_{ij_1}^{(1)} (h_2^{(1)}(v_{j_1}) - h_2^{(1)}(v_i)) \\ \quad + \sigma_2 D_v^{(2)} \sum_{j_1=1}^N \sum_{j_2=1}^N A_{ij_1 j_2}^{(2)} (h_2^{(2)}(v_{j_1}, v_{j_2}) - h_2^{(2)}(v_i, v_i)) \end{cases} \quad (18)$$

where  $h_1^{(1)}(u)$  and  $h_2^{(1)}(v)$  encode the first order interaction, while  $h_1^{(2)}(u_1, u_2)$  and  $h_2^{(2)}(v_1, v_2)$  model the second order coupling. We again assume the existence of a homogeneous solution  $(u_i, v_i) = (u^*, v^*)$  and assume it to be stable once we silence both the pairwise coupling,  $P = 1$ , and the high-order one,  $P > 1$ . To study its stability under spatially dependent perturbations, we can follow the derivation presented in the previous section (see also [21]), that ultimately relies on the computation of a Master Stability Function [30] in a setting involving a stationary equilibrium and high-order coupling.

Let us introduce again the perturbation vector  $\vec{\xi} = (\delta u_1, \delta v_1, \dots, \delta u_N, \delta v_N)^\top$ , where  $\delta u_i = u_i - u^*$  and  $\delta v_i = v_i - v^*$ , then one can straightforwardly show that it evolves according to

$$\frac{d}{dt} \vec{\xi} = (\mathbb{I}_N \otimes \mathbf{J}_0 + \sigma_1 \mathbf{L}^{(1)} \otimes \mathbf{J}_{H^{(1)}} + \sigma_2 \mathbf{L}^{(2)} \otimes \mathbf{J}_{H^{(2)}}) \vec{\xi} \quad (19)$$

where  $\mathbf{J}_{H^{(2)}} = \begin{pmatrix} \partial_{u_1} h_1^{(2)}(u^*, u^*) + \partial_{u_2} h_1^{(2)}(u^*, u^*) & 0 \\ 0 & \partial_{v_1} h_2^{(2)}(v^*, v^*) + \partial_{v_2} h_2^{(2)}(v^*, v^*) \end{pmatrix}$  and  $\mathbf{L}^{(2)}$  represents a generalized Laplacian matrix [21] accounting for the three-body interactions, whose elements are given by

$$\mathbf{L}_{ij}^{(2)} = \begin{cases} -\sum_{j,k=1}^N A_{ijk}^{(2)} & \text{for } i = j \\ \sum_{k=1}^N A_{ijk}^{(2)} & \text{for } i \neq j \end{cases} \quad (20)$$

In the following, we will examine different cases of coupling: first, in section IV A, the so called natural coupling [21, 31], which allows an analytical treatment of the problem, but does not permit to fully unveil the potential of high-order terms. The latter will be fully exploited in section IV B, where we will present two special cases of high-order structures in which, despite the general form of the coupling functions, a complete analytical study can be performed. Finally, in section IV C the scenario where both the coupling and the topology are general will be dealt with.

##### A. Natural coupling

A largely used assumption on the coupling terms  $\vec{h}^{(d)}$ , is that once they are evaluated on the synchronous manifold, they return the same value given by  $\vec{h}^{(1)}$ , more precisely

$$\vec{h}^{(d)}(\vec{x}, \dots, \vec{x}) = \dots = \vec{h}^{(2)}(\vec{x}, \vec{x}) = \vec{h}^{(1)}(\vec{x})$$

Such condition is known in the literature as *natural coupling* [21]. In the present framework this implies that

$$h_1^{(2)}(u, u) = h_1^{(1)}(u) \text{ and } h_2^{(2)}(v, v) = h_2^{(1)}(v)$$

To compare the case  $P > 1$  with the one presented for  $P = 1$ , we consider cubic nonlinearities both in the first and in the second order terms. In particular, we set  $h_1^{(1)}(u) = D_u^{(1)}u^3$  and  $h_2^{(1)}(v) = D_v^{(1)}v^3$  for the two-body coupling, while we take  $h_1^{(2)}(u_1, u_2) = D_u^{(2)}u_1^2u_2$  and  $h_2^{(2)}(v_1, v_2) = D_v^{(2)}v_1^2v_2$ , for the three-body interaction. Note that this choice for the coupling functions satisfies the condition of natural coupling as long as

$$D_u^{(1)} = D_u^{(2)} \text{ and } D_v^{(1)} = D_v^{(2)} \quad (21)$$

Given these coupling functions, we can rewrite Eq. (18) as

$$\begin{cases} \dot{u}_i = f_1(u_i, v_i) + \sigma_1 D_u^{(1)} \sum_{j_1=1}^N A_{ij_1}^{(1)}(u_{j_1}^3 - u_i^3) + \sigma_2 D_u^{(2)} \sum_{j_1=1}^N \sum_{j_2=1}^N A_{ij_1 j_2}^{(2)}(u_{j_1}^2 u_{j_2} - u_i^3) \\ \dot{v}_i = f_2(u_i, v_i) + \sigma_1 D_v^{(1)} \sum_{j_1=1}^N A_{ij_1}^{(1)}(v_{j_1}^3 - v_i^3) + \sigma_2 D_v^{(2)} \sum_{j_1=1}^N \sum_{j_2=1}^N A_{ij_1 j_2}^{(2)}(v_{j_1}^2 v_{j_2} - v_i^3) \end{cases} \quad (22)$$

Again, to study the stability of the homogeneous solution  $(u_i, v_i) = (u^*, v^*)$  we linearize Eq. (22). By resorting to the natural coupling assumption we can conclude that  $\mathbf{J}_{H^{(1)}} = \mathbf{J}_{H^{(2)}}$  and thus rewrite Eq. (19) as follows:

$$\frac{d}{dt} \vec{\xi} = \left[ \mathbb{I}_N \otimes \mathbf{J}_0 + \left( \sigma_1 \mathbf{L}^{(1)} + \sigma_2 \mathbf{L}^{(2)} \right) \otimes \mathbf{J}_{H^{(1)}} \right] \vec{\xi} \quad (23)$$

where

$$\mathbf{J}_{H^{(1)}} = 3 \begin{bmatrix} (u^*)^2 D_u^{(1)} & 0 \\ 0 & (v^*)^2 D_v^{(1)} \end{bmatrix}$$

and  $\vec{\xi} = (\delta u_1, \delta v_1, \dots, \delta u_N, \delta v_N)^\top$ , with  $\delta u_i = u_i - u^*$  and  $\delta v_i = v_i - v^*$ . Let us observe that Eq. (23) recalls the similar result obtained in [20]. However, the mathematical framework here proposed is more general, as it allows to study a broader class of high-order couplings (see Appendix A for more details).

The natural coupling assumption allowed us to introduce an “effective” Laplacian that encodes the high-order structure into a weighted network, whose weights are self-consistently determined,  $\mathbf{M} = \sigma_1 \mathbf{L}^{(1)} + \sigma_2 \mathbf{L}^{(2)}$ . Resorting to the eigenbasis for  $\mathbf{M}$  one can make one step further and project the  $2N \times 2N$  linear system onto  $N$  linear systems of size  $2 \times 2$  depending each one on a single eigenvalue,  $\Lambda_\alpha$ , of  $\mathbf{M}$ , more precisely

$$\frac{d}{dt} \begin{pmatrix} \delta \hat{u}_\alpha \\ \delta \hat{v}_\alpha \end{pmatrix} = [\mathbf{J}_0 + \Lambda_\alpha \mathbf{J}_{H^{(1)}}] \begin{pmatrix} \delta \hat{u}_\alpha \\ \delta \hat{v}_\alpha \end{pmatrix} := \mathbf{J}^{(\alpha)} \begin{pmatrix} \delta \hat{u}_\alpha \\ \delta \hat{v}_\alpha \end{pmatrix} \quad \forall \alpha = 1, \dots, N \quad (24)$$

where again  $\delta \hat{u}_\alpha = \sum_i \delta u_i \phi_{\alpha,i}$ , resp.  $\delta \hat{v}_\alpha = \sum_i \delta v_i \phi_{\alpha,i}$ , is the projection of  $\delta u_i$ , resp.  $\delta v_i$ , on the eigenvector  $\phi_\alpha$ .

Let us observe that the latter equation is formally the same as the one obtained in the case of pairwise interactions (10) and thus the same analysis follows, except that now the eigenvalues depend on the coupling strengths. In Fig. 2, we show the dispersion relation and an example of Turing patterns for the Brusselator model (Eqs. (12)). Let us notice that the blue curve (left panel Fig. 2) has been computed by considering  $\Lambda_\alpha$  to be a continuous variable, corresponding thus to the dispersion relation for a system defined on a continuous support with periodic boundary conditions. Having fixed the topology of binary interactions and the high-order ones, hence the matrices  $\mathbf{L}^{(1)}$  and  $\mathbf{L}^{(2)}$ , we can vary the coupling strengths  $\sigma_1$  and  $\sigma_2$ , and thus letting  $\Lambda_\alpha$  “to slide” along this curve (cyan dots). Stated differently, the Turing instability can be obtained (or repressed) by simply changing the coupling and keeping the remaining part of the model unchanged.

## B. Regular topologies

Let us now relax the natural coupling assumption by setting different diffusion coefficients at the different considered order, i.e.,  $D_u^{(1)} \neq D_u^{(2)}$  and  $D_v^{(1)} \neq D_v^{(2)}$ , but keeping the same form for the coupling functions. Namely we take  $h_1^{(1)}(u) = D_u^{(1)}u^3$  and  $h_2^{(1)}(v) = D_v^{(1)}v^3$  for the two-body coupling, while we take  $h_1^{(2)}(u_1, u_2) = D_u^{(2)}u_1^2u_2$  and  $h_2^{(2)}(v_1, v_2) = D_v^{(2)}v_1^2v_2$  for the three-body coupling. It would also be possible to adopt different coupling functional forms for each order, but, as it will be clear in the following, it is more interesting to focus on the diffusion coefficients, the latter having a key role in the Turing mechanism of



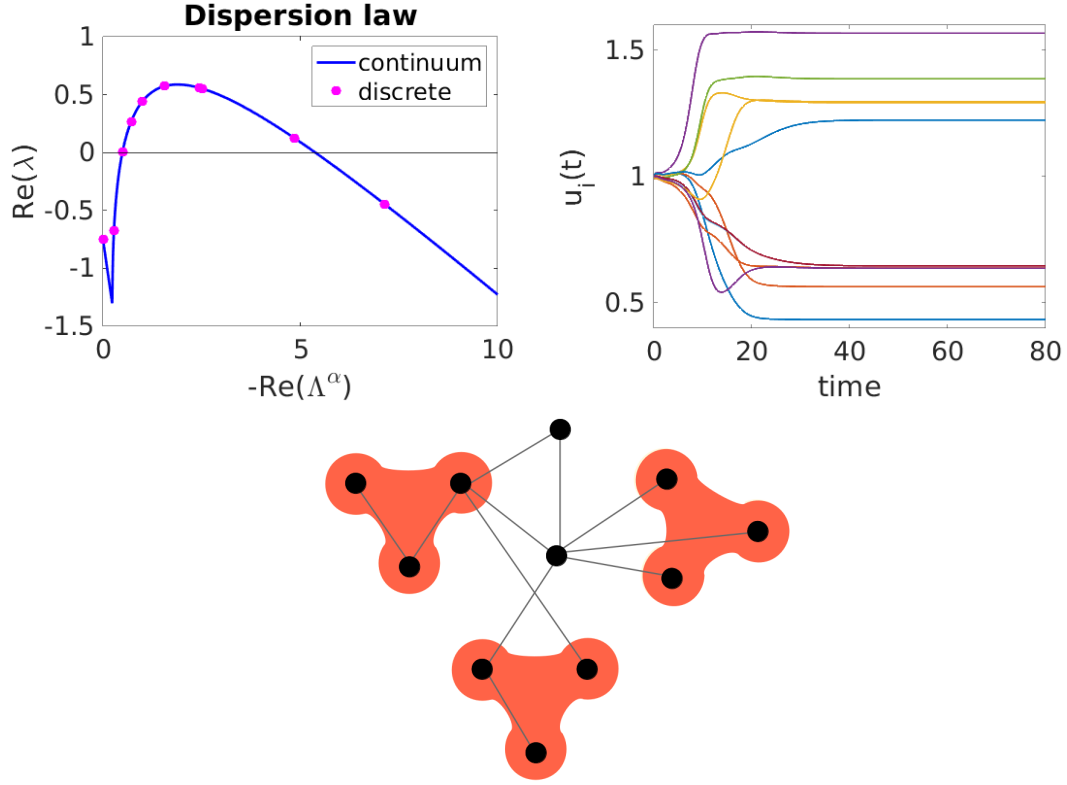


Figure 2. *Turing instability with nonlinear diffusion in high-order structures.* Brusselator model with  $b = 3$ ,  $c = 3.5$ ,  $D_u^{(1,2)} = 0.1$ ,  $D_v^{(1,2)} = 2$ ,  $\sigma_{1,2} = 1$ ; the initial perturbation is  $\sim 10^{-2}$ . On the upper left panel, the dispersion law: the blue line is the continuous one, while the cyan dots indicate the discrete counterpart. On the upper right panel, Turing patterns for the  $u$  species. On the bottom panel the hypergraph on which the system has been simulated: 11 nodes, 11 links and 3 2-hyperedges (i.e., triangles).

pattern formation. Nevertheless, the following analysis could be easily extended to a setting in which coupling functions have different form, as long as they remain diffusive-like.

The starting point for the linear stability analysis is again Eq. (19); however, because  $\mathbf{J}_{H^{(1)}} \neq \mathbf{J}_{H^{(2)}}$  one cannot simplify the latter equation to obtain the analogous of (23). In the same spirit of simplifying the stability equation, we can observe that in general the two Laplacians do not commute and thus they cannot be simultaneously diagonalized. In conclusion one cannot determine a single equation, depending on the spectrum of the involved Laplacian matrices, and proceed with the analysis as done in the case of the Master Stability Function. The numerical computation of the eigenvalues of the  $2N \times 2N$  linear system would not allow a clear understanding of the role of the involved parameters.

There are however some high-order structures allowing for a complete analytical description: this is the case whenever the high-order Laplacian matrix is a multiple of the network Laplacian one. We will call topologies with the above property *regular topologies*. Tetrahedra or icosaedra are examples of regular topologies as well as the *triangular lattice with periodic boundary conditions*, i.e., a 2-torus paved with triangles, that we hereby analyze in details. Let us observe that we assume the nodes forming a triangle (of first order interactions) to be also part of a three-body interaction; for this reason we will call it *triangular 2-lattice*. In this case, each node interacts with its six neighbors through six two-body interactions and six three-body interactions.

Let us consider a triangular 2-lattice of  $N$  nodes, where each node  $i$  has 6 incident links. Its first order Laplacian will then be

$$\mathbf{L}_{ij}^{(1)} = \begin{cases} -6 & \text{if } i = j \\ A_{ij}^{(1)} & \text{otherwise} \end{cases}$$

If now each node will also have 6 incident triangles, we have that

$$\sum_{j,k=1}^N A_{ijk}^{(2)} = 2 \cdot 6 = 12 \quad \text{and} \quad \sum_{k=1}^N A_{ijk}^{(2)} = 2A_{ij}^{(1)}$$

From the definition of the second order Laplacian, Eq. (20), we obtain the relation

$$\mathbf{L}^{(2)} = 2\mathbf{L}^{(1)} \quad (25)$$

hence the two Laplacians can be both diagonalized through the eigenvectors of  $\mathbf{L}^{(1)}$ . Eq. (19) now takes the form

$$\frac{d}{dt}\vec{\xi} = \left( \mathbb{I}_N \otimes \mathbf{J}_0 + \mathbf{L}^{(1)} \otimes (\sigma_1 \mathbf{J}_{H^{(1)}} + 2\sigma_2 \mathbf{J}_{H^{(2)}}) \right) \vec{\xi} \quad (26)$$

We can then proceed in projecting on the eigenvectors of  $\mathbf{L}^{(1)}$ , by obtaining

$$\frac{d}{dt} \begin{pmatrix} \delta \hat{u}_\alpha \\ \delta \hat{v}_\alpha \end{pmatrix} = [\mathbf{J}_0 + \Lambda_\alpha (\sigma_1 \mathbf{J}_{H^{(1)}} + 2\sigma_2 \mathbf{J}_{H^{(2)}})] \begin{pmatrix} \delta \hat{u}_\alpha \\ \delta \hat{v}_\alpha \end{pmatrix} \quad \forall \alpha = 1, \dots, N \quad (27)$$

which is analogous to Eq. (24) due to the properties of the topology. The Laplacian eigenvalues  $\Lambda_\alpha$  can be effectively replaced by a continuous parameter, which is the continuous spectrum of the corresponding diffusion operator, allowing us to have an analytical expression of the dispersion law. *Mutatis mutandis*, the above analysis stands for all regular topologies.

Let us point out that the assumption of  $\mathbf{L}^{(2)}$  to be proportional to  $\mathbf{L}^{(1)}$  allows to emphasize effects of high-order interactions which would not be possible under the natural coupling assumption. In fact, one can deal with sets of parameters which do not allow the formation of patterns by considering the sole pairwise interactions, i.e., condition (17) would not be satisfied,  $(v^*)^2 D_v^{(1)} < (u^*)^2 D_u^{(1)}$ , and thus patterns could not develop, but the appropriate values of the second order couplings would make possible the Turing instability,  $(v^*)^2 D_v^{(2)} > (u^*)^2 D_u^{(2)}$ . This is the case shown in Fig. 3, where we can observe the dispersion law and an example of a pattern obtained with the Brusselator model on a triangular 2-lattice of 16 nodes; we notice that, while the pairwise case (purple dashed line) never allows instability, the high-order one yields Turing patterns. Let us remark that the dispersion law is a function of the Laplacian ( $\mathbf{L}^{(1)}$ ) spectrum.

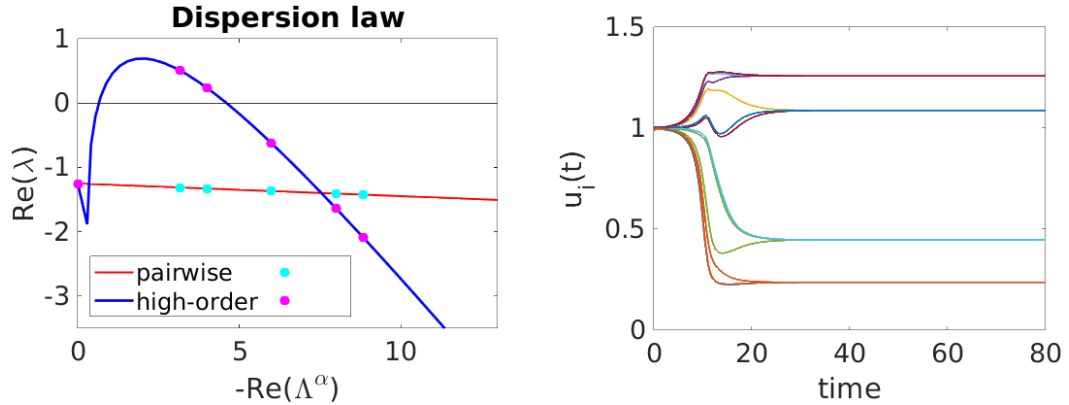


Figure 3. Triangular 2-lattice of 16 nodes with periodic boundary conditions; Brusselator model with  $b = 5.5$ ,  $c = 7$ ,  $D_u^{(1)} = 1$ ,  $D_v^{(1)} = 0.5$ ,  $D_u^{(2)} = 0.1$ ,  $D_v^{(2)} = 1$ ,  $\sigma_1 = 0.01$  and  $\sigma_2 = 1$ ; the initial perturbation is  $\sim 10^{-2}$ . In the left panel, the dispersion law for the high-order case (blue line and magenta dots) compared with the case where only pairwise interactions are present (purple dashed line). In the right panel, an example of a Turing pattern for the  $u$  species.

Let us stress that it is also possible to find the opposite case, in which pairwise interactions would normally give rise to Turing patterns, but the presence of high-order ones annihilates them and stabilizes the system, as exemplified in Fig. 4.

In the next section, we will study the general case in which the absence of natural coupling and a generic high-order structure limits the analytical study, requiring us to resort to numerical simulations. But before that, let us examine a particular case of regular topology, where the Laplacians of all orders can be diagonalized simultaneously: the *all-to-all coupling*, where every possible  $d$ -body interaction is active. When dealing with such coupling, the analysis is not restricted to some orders of interactions but can be extended to all of them. Nonetheless, without further ado, let us again restrict the analysis to first- and second-order interactions. For  $N$  interconnected systems we have  $\mathbf{L}^{(2)} = (N - 2)\mathbf{L}^{(1)}$  (see [21] for a detailed analysis); let us observe that this is again a case where  $\mathbf{L}^{(2)}$  is proportional to  $\mathbf{L}^{(1)}$ , however here the proportionality constant depends on the system size. Based on the above, Eq. (19) can be rewritten as

$$\frac{d}{dt}\vec{\xi} = \left( \mathbb{I}_N \otimes \mathbf{J}_0 + \sigma_1 \mathbf{L}^{(1)} \otimes \left( \mathbf{J}_{H^{(1)}} + \frac{\sigma_2}{\sigma_1} (N - 2) \mathbf{J}_{H^{(2)}} \right) \right) \vec{\xi} \quad (28)$$

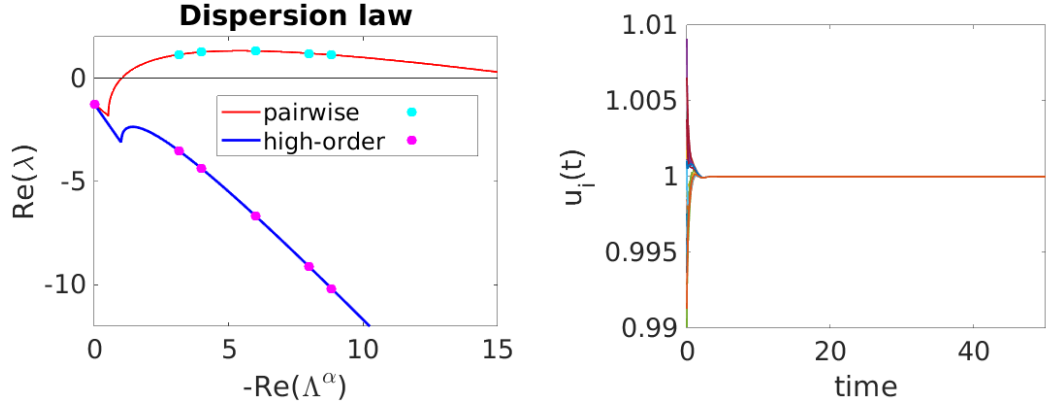


Figure 4. Triangular 2-lattice of 16 nodes with periodic boundary conditions; Brusselator model with  $b = 5.5$ ,  $c = 7$ ,  $D_u^{(1)} = 0.1$ ,  $D_v^{(1)} = 1.5$ ,  $D_u^{(2)} = 1$ ,  $D_v^{(2)} = 0.5$ ,  $\sigma_1 = 0.7$  and  $\sigma_2 = 0.2$ ; the initial perturbation is  $\sim 10^{-2}$ . In the left panel, the dispersion law for the high-order case (blue line and magenta dots) compared with the case where only pairwise interactions are present (purple dashed line). As the high-order dispersion law is always negative, there is no emergence of Turing patterns, as also shown in the right panel for the  $u$  species.

Projecting again on the eigenvectors of  $\mathbf{L}^{(1)}$  we obtain

$$\frac{d}{dt} \begin{pmatrix} \delta u_\alpha \\ \delta v_\alpha \end{pmatrix} = \left[ \mathbf{J}_0 + \sigma_1 \Lambda_\alpha \left( \mathbf{J}_{H^{(1)}} + \frac{\sigma_2}{\sigma_1} (N-2) \mathbf{J}_{H^{(2)}} \right) \right] \begin{pmatrix} \delta u_\alpha \\ \delta v_\alpha \end{pmatrix} \quad \forall \alpha = 1, \dots, N$$

Let us observe that  $\Lambda_\alpha = \{0, N\}$ , hence the dispersion law depends on the number of nodes. The above equation indicates that it is possible to decompose the instability modes.

For a given value of  $N$ , having fixed the ratio  $\sigma_2/\sigma_1$ , we can vary the value of  $\sigma_1$ , thus generating a continuous curve. Observe that such a curve allows us to check for the onset of Turing instability on the “all-to-all” configuration. Indeed, when the curve is negative Turing instability cannot occur for any value of  $\sigma_1$ , while Turing patterns can emerge in the opposite case. Hence, the continuous curve, as function of a parameter  $\gamma = \sigma_1 \Lambda_\alpha$ , can be subsumed in the framework of the Master Stability Function approach [30].

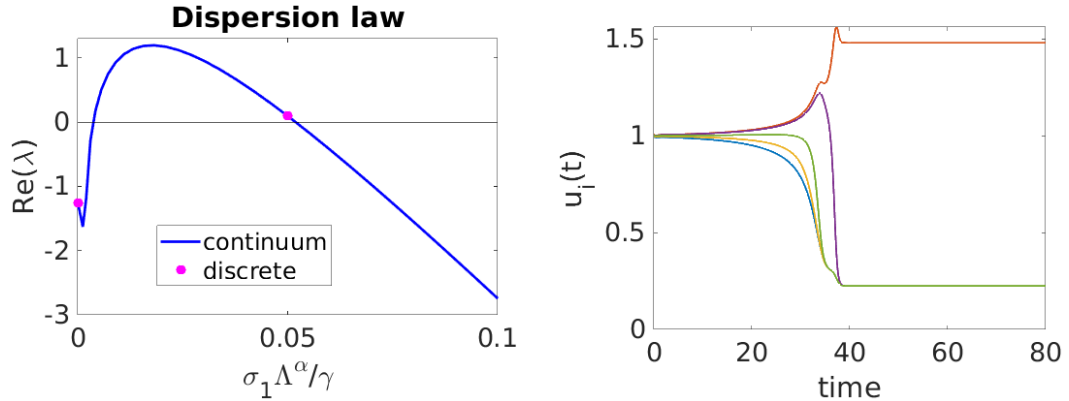


Figure 5. All-to-all 2-hypergraph of 5 nodes; Brusselator model with  $b = 5.5$ ,  $c = 7$ ,  $D_u^{(1)} = 1$ ,  $D_v^{(1)} = 0.1$ ,  $D_u^{(2)} = 0.07$ ,  $D_v^{(2)} = 1$ ,  $\sigma_1 = 0.01$  and  $\sigma_2 = 1$ ; the initial perturbation is  $\sim 10^{-2}$ . On the left panel, the discrete dispersion law; note that the continuous curve is a fictitious dispersion law, but it is a Master Stability Function, as explained in the text; for this reason the continuous curve can be thought as a function of a parameter  $\gamma$ . On the right panel, an example of a Turing pattern for the  $u$  species.

To provide a numerical example, let us consider an ensemble of  $N$  Brusselator systems interacting in the all-to-all configuration, with  $h_1^{(1)} = D_u^{(1)} u^3$ ,  $h_2^{(1)} = D_v^{(1)} v^3$ ,  $h_1^{(2)}(u_1, u_2) = D_u^{(2)} u_1^2 u_2$  and  $h_2^{(2)}(v_1, v_2) = D_v^{(2)} v_1^2 v_2$ , and with the values of the diffusion coefficients set such that the coupling functions do not satisfies the natural coupling condition. In Fig. 5, we report a case analogous to that displayed in Fig. 3, namely patterns emerge due to high-order interaction. Also in this case, with the appropriate coupling functions we can obtain the opposite situation, i.e., high-order interactions annihilate patterns, which would otherwise emerge with the sole pairwise ones.

### C. General topologies

Let us now focus on the most general case, in which arbitrary high-order topologies are considered and the coupling is not restricted to the natural coupling form. Following the same reasoning of the previous section, we use different diffusion coefficients, while the coupling functions remain of the same form.

In such setting, we cannot have an analytical form of the dispersion law, because neither the Laplacians nor the matrices  $J_{H^{(d)}}$  can be diagonalized simultaneously. Hence, we will resort to numerical simulations to determine the onset of the Turing instability.

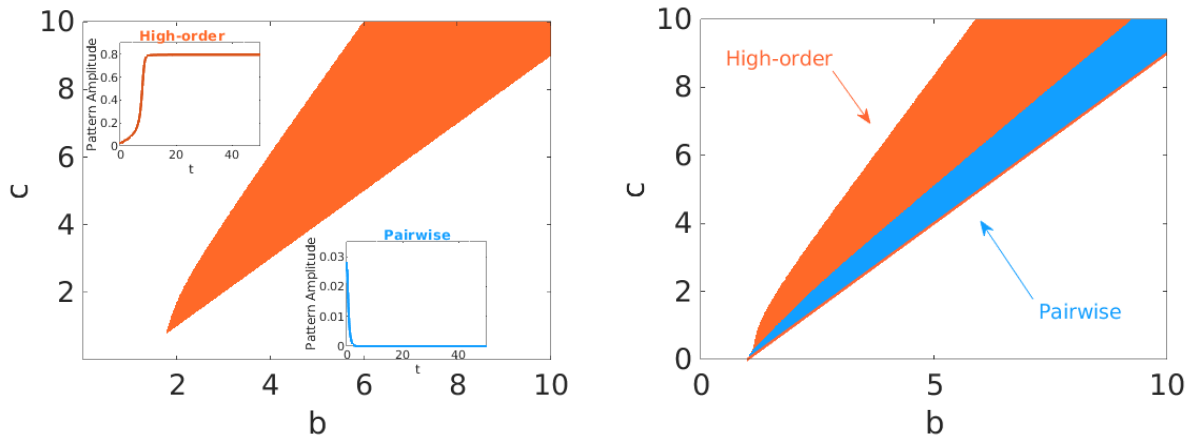


Figure 6. Left panel: Brusselator model with  $D_u^{(1)} = 1$ ,  $D_v^{(1)} = 0.5$ ,  $D_u^{(2)} = 0.1$ ,  $D_v^{(2)} = 2$ ,  $\sigma_1 = 0.1$  and  $\sigma_2 = 1$ . The setting does not allow for Turing patterns when only pairwise interaction are considered, hence to obtain the instability region we need to include also high-order (three-body) interactions (the region of parameters where patterns are obtained is shown in orange). Numerical simulations of the system with  $b = 5.5$  and  $c = 7$  without (resp. with) high-order terms show that Turing patterns are not obtained (resp. are obtained) as confirmed by the total pattern amplitude [13] in blue (resp. orange) on the lower (resp. upper) inset. Right panel: Brusselator model with  $D_u^{(1)} = 0.1$ ,  $D_v^{(1)} = 0.5$ ,  $D_u^{(2)} = 0.01$ ,  $D_v^{(2)} = 1$ ,  $\sigma_1 = 0.2$  and  $\sigma_2 = 1$ . The instability region when only pairwise interactions are considered is depicted in blue, while in orange the one obtained when also high-order ones are active; note that the blue region is a subset of the orange one. For both panels, the initial perturbation is  $\sim 10^{-2}$  and the hypergraph is that of in Fig. 2.

Based on the above discussion, we thus performed a dedicated numerical analysis of this scenario that allows us to fully exploit the presence of high-order terms. The results are reported in Fig. 6 where we show the parameters region associated to a Turing instability in the case of the Brusselator model with cubic coupling, see Eq. (22). On the left panel, the first order diffusion coefficients (i.e., pairwise) do not allow Turing instability (since  $(v^*)^2 D_v^{(1)} > (u^*)^2 D_u^{(1)}$ ), on the other hand the presence of high-order diffusion with a suitable choice of the weights  $\sigma_i$  allows the formation of patterns. On the right panel, instead, Turing instability arises even in the pairwise setting, but many-body interaction are still beneficial as they yield a larger region of parameters for which patterns can be obtained.

Let us conclude by remarking that, in analogy with the setting studied in the previous section (i.e., regular topologies), it is also possible to find couplings such that high-order interaction hamper the formation of Turing patterns, which would normally arise when the interactions are limited to be pairwise.

### V. DISCUSSION

In this work we have formulated a general theory to study the emergence of Turing patterns for dynamical systems high-order interactions. Our framework goes beyond the one recently proposed [20] that, as shown in the Appendix, can be recovered as a special case of the theory hereby developed. Our framework is inspired by the work of [21] dealing with synchronization in high-order structures and allows to obtain patterns in settings where it would be otherwise impossible. At the same time it also permits to suppress the instability which would occur with only pairwise interactions, depending on the desired applications. We have shown that including diffusion terms from high-order interactions may either widen the region of parameters where patterns occur, or, on the contrary, reduce its extension. This can be achieved acting only on the diffusion coefficients but also using different coupling functions. The detailed analytical study we performed provided us a clear understanding of the role of the model parameters as well as of the high-order topology in the pattern emergence. This further flexibility in the choice of the parameters can shed light on the fine tuning problem [32] and benefit the field of optimal control of patterns [33–35]. In fact,

one could choose the appropriate coupling functions and/or diffusion coefficients in order to obtain the desired inhomogeneous state.

A natural extension of our framework would be to study Turing (wave) instability emerging from a limit cycle: in fact, it has been shown that a similar instability mechanism can occur also when the homogeneous stable state is a limit cycle [36, 37]. In many applications where it is important to control the emergence of synchronization, such as neuroscience, our theory could provide to be extremely useful. Moreover, exploring the onset of Turing patterns in the newly developed framework of  $M$ -directed hypergraphs [38] could provide another interesting direction where to focus the attention in future works.

#### Acknowledgements

The authors would like to thank Lorenzo Giambagli and Lucia Valentina Gambuzza for useful discussions and feedback. R.M. is supported by a FRIA-FNRS PhD fellowship, Grant FC 33443, funded by the Walloon region. R.M. acknowledges the Erasmus+ program for funding his visit in the group of Professor M.F.

- 
- [1] Anderson PW. 1972 More is different. Broken symmetries and the nature of hierarchical structure of science. *Physical Review Letters* **177**.
  - [2] Turing AM. 1952 The chemical basis of morphogenesis. *Phil. Trans. R. Soc. Lond. B* **237**, 37.
  - [3] Gierer A, Meinhardt H. 1972 A theory of biological pattern formation. *Kybernetik* **12**, 30–39.
  - [4] Murray JD. 2001 *Mathematical biology II: Spatial models and biomedical applications*. Springer-Verlag.
  - [5] Castets V, Dulos E, Boissonade J, De Kepper P. 1990 Experimental evidence of a sustained standing Turing-type nonequilibrium chemical pattern. *Phys. Rev. Lett.* **64**, 2953.
  - [6] De Kepper P, Castets V, Dulos E, Boissonade J. 1991 Turing-type chemical patterns in the chlorite–iodide–malonic acid reaction. *Physica D* **49**.
  - [7] Goras L, Chua L. 1995 Turing patterns in CNNs. II. Equations and behaviors. *IEEE Transactions on Circuits and Systems I: Fundamental Theory and Applications* **42**, 612–626.
  - [8] Buscarino A, Corradino L, Fortuna L, Frasca M, Chua L. 2016 Turing patterns in memristive cellular nonlinear networks. *IEEE Transactions on Circuits and Systems I: Regular Papers* **63**, 1222–1230.
  - [9] Biancalani T, Di Patti F, Fanelli D. 2010 Stochastic Turing patterns in the Brusselator model. *Phys. Rev. E* **4**, 046215.
  - [10] Zemskov EP, Horsthemke W. 2016 Diffusive instabilities in hyperbolic reaction-diffusion equations. *Phys. Rev. E* **93**, 032211.
  - [11] Carletti T, Muolo R. 2021 Finite propagation enhances Turing patterns in reaction–diffusion networked systems. *Journal of Physics: Complexity* **2**, 045004.
  - [12] Othmer HG, Scriven LE. 1971 Instability and dynamic pattern in cellular networks. *J. Theor. Biol.* **32**, 507.
  - [13] Nakao H, Mikhailov AS. 2010 Turing patterns in network-organized activator-inhibitor systems. *Nature Physics* **6**, 544.
  - [14] Pastor-Satorras R, Vespignani A. 2010 Patterns of complexity. *Nature Physics* **6**, 480.
  - [15] Asllani M, Carletti T, Fanelli D, Maini PK. 2020 A universal route to pattern formation in multicellular systems. *The European Physics Journal B* **93**.
  - [16] Asllani M, Challenger JD, Pavone FS, Sacconi L, Fanelli D. 2014 The theory of pattern formation on directed networks. *Nature Communication* **5**.
  - [17] Muolo R, Asllani M, Fanelli D, Maini PK, Carletti T. 2019 Patterns of non-normality in networked systems. *Journal of Theoretical Biology* **480**, 81.
  - [18] Battiston F, Cencetti G, Iacopini I, Latora V, Lucas M, Patania A, Young JG, Petri G. 2020 Networks beyond pairwise interactions: structure and dynamics. *Physics Reports*.
  - [19] F B, et al.. 2021 The physics of higher-order interactions in complex systems. *Nature Physics* **17**, 1093–1098.
  - [20] Carletti T, Fanelli D, Nicoletti S. 2020 Dynamical systems on hypergraphs. *Journal of Physics: Complexity* **1**, 035006.
  - [21] Gambuzza LV, Di Patti F, Gallo L, Lepri S, Romance M, Criado R, Frasca M, Latora V, Boccaletti S. 2021 Stability of synchronization in simplicial complexes. *Nature communications* **12**, 1–13.
  - [22] Kumar N, Horsthemke W. 2010 Turing bifurcation in a reaction-diffusion system with density-dependent dispersal. *Physica A* **389**, 1812–1818.
  - [23] Gambino F, Lombardo M, Sammartino M, Sciacca V. 2013 Turing pattern formation in the Brusselator system with nonlinear diffusion. *Phys. Rev. E* **88**, 042925.
  - [24] Sadighi A, Ganji D. 2007 Exact solutions of nonlinear diffusion equations by variational iteration method. *Comp. Math. Appl.* **54**, 1112–1121.
  - [25] Newman ME. 2010 *Networks: An Introduction*. Oxford: Oxford University Press.
  - [26] Prigogine I, Nicolis G. 1967 Symmetry breaking instabilities in dissipative systems. *J. Chem. Phys.* **46**, 3542.
  - [27] Boland RP, Galla T, McKane AJ. 2008 How limit cycles and quasi-cycles are related in a system with intrinsic noise. *J. Stat. Mech.* p. P09001.
  - [28] Neuhäuser L, Mellor A, Lambiotte R. 2020 Multibody interactions and nonlinear consensus dynamics on networked systems. *Physical Review E* **101**, 032310.

- [29] Sadighi A, Ganji D. 2007 Exact solutions of nonlinear diffusion equations by variational iteration method. *Computers & Mathematics with Applications* **54**, 1112–1121.
- [30] Pecora LM, Carroll TL. 1998 Master stability functions for synchronized coupled systems. *Physical Review Letters* **80**, 2109.
- [31] Carletti T, Muolo R. 2021 Non-reciprocal interactions enhance heterogeneity. *arXiv preprint arXiv:2112.02549*.
- [32] Haas PA, Goldstein RE. 2021 Turing’s Diffusive Threshold in Random Reaction-Diffusion Systems. *Phys. Rev. Letters* **126**, 238101.
- [33] Hata S, Nakao H, Mikhailov AS. 2012 Global feedback control of Turing patterns in network-organized activator-inhibitor systems. *Eur. Phys. Lett.* **98**, 64004.
- [34] Buscarino A, Corradino C, Fortuna L, Frasca M. 2019 Turing patterns via pinning control in the simplest memristive cellular nonlinear networks. *Chaos* **29**, 103145.
- [35] Gao S, Chang L, Romić I, Wang Z, Jusup M, Holme P. 2022 Optimal control of networked reaction–diffusion systems. *Journal of the Royal Society Interface* **19**, 20210739.
- [36] Challenger J, Fanelli D, Burioni R. 2015 Turing-like instabilities from a limit cycle. *Phys. Rev. E* **92**, 022818.
- [37] Muolo R, Carletti T, Gleeson JP, Asllani M. 2021 Synchronization dynamics in non-normal networks: the trade-off for optimality. *Entropy* **23**, 36.
- [38] Gallo L, Muolo R, Gambuzza LV, Latora V, Frasca M, Carletti T. 2022 Synchronization induced by directed higher-order interactions. *arXiv preprint arXiv:2202.08707*.

### Appendix A: Formalism mapping

In this appendix, we show how the formalism introduced in [20] to study the formation of Turing patterns on hypergraphs can be recovered from the mathematical framework developed in [21] for the analysis of synchronization of chaotic oscillators in simplicial complexes. Note that the latter also applies to the case of hypergraphs, as discussed in [38].

We start from the dynamical system (1). First, we assume the coupling functions  $\vec{g}^{(d)}$  to be in the form

$$\begin{aligned}\vec{g}^{(d)}(\vec{x}_i, \vec{x}_{j_1}, \vec{x}_{j_2}, \dots, \vec{x}_{j_d}) &= \varphi(d+1)[\gamma(\vec{x}_{j_1}) - \gamma(\vec{x}_i) + \dots + \gamma(\vec{x}_{j_d}) - \gamma(\vec{x}_i)] \\ &= \varphi(d+1) \left[ \sum_{n=1}^d \gamma(\vec{x}_{j_n}) - d\gamma(\vec{x}_i) \right]\end{aligned}\quad (\text{A1})$$

where  $\varphi : \mathbb{R} \rightarrow \mathbb{R}$  is a generic function of the number of nodes involved in the high-order interaction, i.e., the size of the hyperedge or of the simplex, while  $\gamma : \mathbb{R}^m \rightarrow \mathbb{R}^m$  is a generic function encoding the contribution of the node state vectors to the coupling. Note that, given the form in Eq. (A1), all the coupling functions are non-invasive. Eq. (1) can be hence rewritten as

$$\begin{aligned}\dot{\vec{x}}_i &= \vec{f}(\vec{x}_i) + \sigma_1 \sum_{j_1=1}^N A_{ij_1}^{(1)} \varphi(2)[\gamma(\vec{x}_{j_1}) - \gamma(\vec{x}_i)] + \\ &+ \sigma_2 \sum_{j_1=1}^N \sum_{j_2=1}^N A_{ij_1 j_2}^{(2)} \varphi(3)[\gamma(\vec{x}_{j_1}) + \gamma(\vec{x}_{j_2}) - 2\gamma(\vec{x}_i)] + \dots \\ &+ \sigma_P \sum_{j_1=1}^N \dots \sum_{j_P=1}^N A_{ij_1 j_2 \dots j_P}^{(P)} \varphi(P+1) \left[ \sum_{n=1}^P \gamma(\vec{x}_{j_n}) - P\gamma(\vec{x}_i) \right]\end{aligned}\quad (\text{A2})$$

Noticing that each adjacency tensor  $A^{(d)}$  is symmetric with respect to its  $d+1$  indices, i.e.,  $A_{ij_1 j_2 \dots j_d}^{(d)} = A_{\pi(i j_1 j_2 \dots j_d)}^{(d)}$ , where  $\pi$  is a generic permutation of the indices, we can simplify the coupling terms, thus writing Eq. (A2) as

$$\begin{aligned}\dot{\vec{x}}_i &= \vec{f}(\vec{x}_i) + \sigma_1 \sum_{j_1=1}^N A_{ij_1}^{(1)} \varphi(2)[\gamma(\vec{x}_{j_1}) - \gamma(\vec{x}_i)] + \\ &+ 2\sigma_2 \sum_{j_1=1}^N \varphi(3)[\gamma(\vec{x}_{j_1}) - \gamma(\vec{x}_i)] \sum_{j_2=1}^N A_{ij_1 j_2}^{(2)} + \dots \\ &+ P\sigma_P \sum_{j_1=1}^N \varphi(P+1)[\gamma(\vec{x}_{j_1}) - \gamma(\vec{x}_i)] \sum_{j_2=1}^N \dots \sum_{j_P=1}^N A_{ij_1 j_2 \dots j_P}^{(P)}\end{aligned}\quad (\text{A3})$$

By recalling the definition [21] of the generalized  $d$ -degree,  $k_{ij}^{(d)}$ , of a link  $(i, j)$ , which represents the number of  $d$ -order structures the link  $(i, j)$  is part of

$$(d-1)!k_{ij}^{(d)} = \sum_{l_2=1}^N \dots \sum_{l_d=1}^N A_{il_1 l_2 \dots l_d}^{(d)} \quad (\text{A4})$$

and by noticing that  $k_{ij}^{(1)} = A_{ij}^{(1)}$ , we can write the equations governing the dynamics of the system as

$$\begin{aligned} \dot{\vec{x}}_i = & \vec{f}(\vec{x}_i) + \sigma_1 \sum_{j=1}^N k_{ij}^{(1)} \varphi(2) \Delta_j + 2\sigma_2 \sum_{j=1}^N k_{ij}^{(2)} \varphi(3) \Delta_j + \dots \\ & + P(P-1)! \sigma_P \sum_{j=1}^N k_{ij}^{(P)} \varphi(P+1) \Delta_j \end{aligned} \quad (\text{A5})$$

where we have relabeled index  $j_1$  as  $j$ , and where we have defined  $\Delta_j = \gamma(\vec{x}_j) - \gamma(\vec{x}_i)$ .

By considering the high-order incidence matrix [20],  $e_{i\alpha}$ , defined as

$$e_{i\alpha} = \begin{cases} 1 & v_i \in E_\alpha \\ 0 & \text{otherwise} \end{cases} \quad (\text{A6})$$

where  $E_\alpha$  can represent either an hyperedge or a simplex, we can now write Eq. (A5) as

$$\begin{aligned} \dot{\vec{x}}_i = & \vec{f}(\vec{x}_i) + \sigma_1 \sum_{j=1}^N \sum_{\alpha: |E_\alpha|=2} e_{i\alpha} e_{j\alpha} \varphi(2) \Delta_j + 2\sigma_2 \sum_{j=1}^N \sum_{\alpha: |E_\alpha|=3} e_{i\alpha} e_{j\alpha} \varphi(3) \Delta_j + \dots \\ & + P! \sigma_P \sum_{j=1}^N \sum_{\alpha: |E_\alpha|=P+1} e_{i\alpha} e_{j\alpha} \varphi(P+1) \Delta_j \end{aligned} \quad (\text{A7})$$

In fact, as for each order  $d$  of the high-order interactions, the factor  $e_{i\alpha} e_{j\alpha}$  is equal to one when both nodes  $i$  and  $j$  belong to  $E_\alpha$ , by summing over all  $j \neq i$ , each summation has exactly  $k_{ij}^{(d)}$  non-zero terms.

Lastly, by assuming the  $d$ -th coupling strength to be  $\sigma_d = \varepsilon/d!$ , we finally obtain

$$\dot{\vec{x}}_i = \vec{f}(\vec{x}_i) + \varepsilon \sum_{j=1}^N \sum_{\alpha} e_{i\alpha} e_{j\alpha} \varphi(|E_\alpha|) [\gamma(\vec{x}_j) - \gamma(\vec{x}_i)] \quad (\text{A8})$$

which recovers the dynamical system analyzed in [20] as we set  $\varphi(|E_\alpha|) = |E_\alpha| - 1$ . Hence, the mathematical framework here considered permits to extend the analysis of Turing pattern formation in hypergraphs, as it allows to consider more general coupling functions.